

# Wetting behavior at the free surface of a liquid gallium-bismuth alloy: An X-ray reflectivity study close to the bulk monotectic point.

P. Huber,<sup>1</sup> O.G. Shpyrko,<sup>1</sup> P.S. Pershan,<sup>1</sup> H. Tostmann,<sup>2</sup> E. DiMasi,<sup>3</sup> B.M. Ocko,<sup>3</sup> and M. Deutsch<sup>4</sup>

<sup>1</sup>*Department of Physics, Harvard University, Cambridge MA 02138*

<sup>2</sup>*Department of Chemistry, University of Florida, Gainesville FL 32611*

<sup>3</sup>*Department of Physics, Brookhaven National Laboratory, Upton NY 11973*

<sup>4</sup>*Department of Physics, Bar-Ilan University, Ramat-Gan 52900, Israel*

(Dated: November 10, 2018)

We present x-ray reflectivity measurements from the free surface of a liquid gallium-bismuth alloy (Ga-Bi) in the temperature range close to the bulk monotectic temperature  $T_{mono} = 222^\circ C$ . Our measurements indicate a continuous formation of a thick wetting film at the free surface of the binary system driven by the first order transition in the bulk at the monotectic point. We show that the behavior observed is that of a complete wetting at a tetra point of solid-liquid-liquid-vapor coexistence.

PACS numbers:

Keywords: wetting, surface, liquid metals, gallium-bismuth, x-ray reflectivity

## I. INTRODUCTION

Interfacial phenomena at the surface of critical systems, particularly at the surfaces of critical binary liquid mixtures, have attracted interest ever since the seminal paper by J.W. Cahn<sup>1</sup> demonstrating the existence of a wetting line, starting at the wetting temperature,  $T_W$ , below the critical point of demixing,  $T_{crit}$ . Initially, experimental efforts were mainly focused on systems dominated by long-range van-der-Waals interactions like methanol-cyclohexane and other organic materials.<sup>23</sup> Only recently have experiments probed the wetting behavior in binary metallic systems, most prominently in gallium-lead (Ga-Pb)<sup>4</sup>, gallium-thallium (Ga-Tl)<sup>5</sup>, and gallium-bismuth (Ga-Bi)<sup>6</sup>. Those systems allow the study of the influence of interactions characteristic of metallic systems on the wetting behavior. By the same token, they allow one to obtain information on the dominant interactions in metallic systems by measurements of the thermodynamics and structure of the wetting films.

This paper reports measurements of the wetting behavior of Ga-Bi close to its monotectic temperature  $T_{mono} = 222^\circ C$ . We first present the bulk phase diagram of Ga-Bi and relate it to the structures at the free surface (liquid-vapor interface) known from optical ellipsometry<sup>6</sup> and recent x-ray reflectivity measurements.<sup>78</sup> The experimental setup is then described, along with some basic principles of the x-ray reflectivity experiment and the data analysis. Finally, our results and the conclusions emerging therefrom are discussed.

## II. BULK AND SURFACE STRUCTURE

The bulk phase diagram of Ga-Bi has been measured by Predel using calorimetric methods<sup>9</sup>, and is shown in Fig. 1. Assuming an overall concentration of 70% Ga, the following behavior is found: Below  $T_{mono}$  (regime I) and at temperatures higher than the melting point of Ga  $T_m(Ga) = 29.5^\circ C$ , solid Bi coexists with a Ga-rich liquid phase. In this regime, previous x-ray measurements have shown that a Gibbs-adsorbed Bi monolayer resides at the free surface.<sup>78</sup> For  $T_{mono} < T < T_{crit}$  (regime II), the bulk phase separates into two immiscible phases, a high density Bi-rich phase and a low density Ga-rich phase. The heavier Bi-rich phase is macroscopically separated from the lighter Ga-rich phase and sinks to the bottom of the sample pan. In temperature regime II, the high density, Bi-rich phase wets the free surface by intruding between the low density phase and the Bi monolayer, in defiance of gravity.<sup>8</sup> Considering that pure Bi has a significantly lower surface tension than pure Ga, the segregation of the Bi-rich phase at the surface is not too surprising. In fact, the thickness of the wetting layer in such a geometry is believed to be limited only by the extra gravitational potential energy paid for having the heavier phase at the top<sup>10</sup>. In regime III, above the consolute point, the bulk is in the homogeneous phase and only a Gibbs-adsorbed Bi monolayer has been found at the free surface.<sup>14</sup>

Despite extensive experimental efforts to relate the bulk phases to the corresponding surface phases, two important questions remain unanswered: What kind of transitions take place at the free surface between regime I and regime II and between regime II and regime III. Here, we focus on the transition between regime I and regime II. Note that these temperature regimes are separated by  $T_{mono}$ , a temperature characterized by the coexistence of the solid Bi, the Bi-rich liquid, the Ga-rich liquid and the vapor.  $T_{mono}$  is therefore a solid-liquid-liquid-vapor

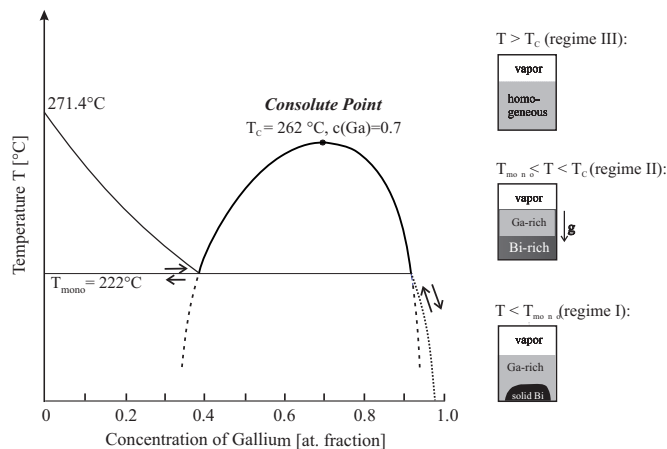


FIG. 1: Bulk Phase diagram of Ga-Bi (Ref.<sup>9</sup>). Bold solid line: liquid-liquid coexistence, dashed line: liquid-liquid coexistence metastable, dotted line: liquid-solid coexistence. On the right: Schematic bulk behavior in the different temperature regimes.

tetra point, at which the solidification of pure bulk Bi takes place. The question is, then, how is this first order bulk transition related to the changes at the surface?

### III. EXPERIMENT

The Ga-Bi alloy was prepared in an inert-gas box using metals with purities greater than 99.9999%. A solid Bi ingot was placed in a Mo pan and oxide formed at the surface was scraped away. Liquid Ga was then added to completely cover the Bi ingot. The sample with an overall Ga amount of 70 at% was transferred through air into an ultrahigh vacuum chamber. After a one day of bake-out, a pressure of  $10^{-10}$  torr was achieved and the residual oxide on the liquid sample was removed by sputtering with  $\text{Ar}^+$  ions, at a sputter current of a 25 microamps and a sputter voltage of 2 kV.

To avoid temperature gradients between the bulk and the surface induced by thermal radiation, a temperature-controlled radiation shield was installed above the sample. The temperature was measured with thermocouples mounted in the bottom of the sample pan and on the radiation shield. The sample pan and the radiation shield temperature were controlled by Eurotherm temperature controllers yielding a temperature stability of  $\pm 0.05^\circ\text{C}$ .

Surface-specific x-ray reflectivity measurements were carried out using the liquid surface reflectometer at beamline X22B at National Synchrotron Light Source with an x-ray wavelength  $\lambda = 1.54\text{\AA}$ . Background and bulk scattering were subtracted from the specular signal by displacing the detector out of the reflection plane. The intensity  $R(q_z)$ , reflected from the surface, is measured as a function of the normal component  $q_z$  of the momentum transfer and yields information about the surface-normal structure of the electron density as given by

$$R(q_z) = R_F(q_z) |\Phi(q_z)|^2 \exp[-\sigma_{cw}^2 q_z^2] \quad (1),$$

where  $R_F(q_z)$  is the Fresnel reflectivity from a flat, infinitely sharp surface, and  $\Phi(q_z)$  is the Fourier transform of the local surface-normal density profile  $\langle \tilde{\rho}(z) \rangle$ :

$$\Phi(q_z) = \frac{1}{\rho_\infty} \int dz \frac{d \langle \tilde{\rho}(z) \rangle}{dz} \exp(iq_z z) \quad (2),$$

with the bulk electron density  $\rho_\infty$  and the critical wave vector  $q_{crit}$ . The exponential factor in Eq. (1) accounts for roughening of the intrinsic density profile  $\langle \tilde{\rho}(z) \rangle$  by capillary waves:

$$\sigma_{cw}^2 = \frac{k_B T}{2\pi\gamma} \ln\left(\frac{q_{max}}{q_{res}}\right) \quad (3),$$

where  $\gamma$  is the macroscopic surface tension of the free surface, and  $\sigma_{cw}$  is the roughness due to thermally excited capillary waves (CW). The CW spectrum is cut off at small  $q_z$  by the detector resolution  $q_{res} = 0.03\text{\AA}^{-1}$  and at large  $q_z$  by the inverse atomic size  $a$ ,  $q_{max} \approx \pi/a$ .<sup>13</sup>

In Expression (1) the validity of the Born approximation is tacitly assumed. Since the features in  $R/R_F$  characteristic of the thick wetting film appear close to the critical wavevector  $q_c = 0.049\text{\AA}^{-1}$  of the Ga-rich subphase, where the Born approximation is no longer valid, we had to resort to Parratt's dynamical formalism<sup>12</sup> for  $q_z$  less than  $0.25\text{\AA}^{-1}$ . Details of this analysis will be reported elsewhere.<sup>14</sup>

### IV. RESULTS

Fig. 2a shows the reflectivity at three temperatures: well below  $T_{mono}$  at  $T = 205^\circ\text{C}$  (regime I), well above  $T_{mono}$  at  $T = 222.5^\circ\text{C}$  (regime II) and at an intermediate temperature  $T = 220^\circ\text{C}$ . Due to the loss of phase information (Eq. 1) the interesting electron density profiles

cannot be obtained directly from the measurement. One has to resort to the widely accepted method of adapting a physically motivated model for the electron density profile and fitting its Fourier transform to the experimentally determined  $R/R_F$ . The resulting electron density profiles for the different temperatures are depicted in Fig. 2b and the corresponding fits to  $R/R_F$  can be seen as solid lines in Fig. 2a.

At  $T = 205^\circ\text{C}$   $R/R_F$  (Fig. 2a, diamonds) shows a pronounced maximum centered around  $q_z = 0.8$ . This maximum is indicative of a high electron density surface of the alloy and a previous analysis indicates that it is compatible with the segregation of a monolayer of pure Bi at the liquid-vapor interface of the bulk.

The normalized reflectivity at  $T = 222.5^\circ\text{C}$  (solid circles) shows two peaks (Kiessig fringes) characteristic of a Bi-rich wetting film  $\approx 12\text{\AA}$  thick. This thickness is in good agreement with electron microscopy measurements on Ga-Bi alloy surfaces in the same temperature regime.<sup>6</sup> The interfacial roughness between the Bi-rich and the Bi-poor phase, indicated by the Kiessig fringes, is  $\approx 12\text{\AA}$ . Additionally,  $R/R_F$  seems to exhibit an increased intensity around  $q_z \approx 0.1$ . The monolayer of pure Bi is still present at the surface in regime II, while the Bi-rich wetting film has formed between it and the Ga-rich subphase.

The reflectivity at the intermediate temperature  $220.0^\circ\text{C}$  (Fig. 2a, open circles) still exhibits a maximum at low  $q_z$ . However, compared to the peak at  $T = 205^\circ\text{C}$  it is now shifted to higher  $q_z$ . The corresponding electron density profile, depicted in Fig. 2b as the dashed line, indicates a highly diffuse, thin film of a Bi-enrichment between the monolayer and the Ga-rich subphase.

To obtain further information about the temperature dependent transition between the different regimes, we performed temperature-dependent reflectivity measurements at a fixed  $q_z$  in a temperature range close to  $T_{mono}$ . These measurements are shown in the following as T-scans. As can be seen in Fig. 2a the reflectivities in the two regimes differ distinctly in the low  $q_z$  part, and somewhat less in the higher  $q_z$ -part. Due to the high sensitivity of the reflectivity to temperature dependent sample height changes at low  $q_z$ , we carried out measurements at a relatively high  $q_z = 0.8\text{\AA}^{-1}$ .

A T-scan while cooling (heating) with a cooling (heating) rate of  $1^\circ\text{C}/\text{hour}$  between  $226^\circ\text{C}$  and  $210^\circ\text{C}$  is shown in Fig. 3. For temperatures higher than  $T_{mono}$  the reflectivity stays constant. Upon  $T$  reaching  $T_{mono}$  the intensity starts rising continuously. When reaching  $210^\circ\text{C}$  the x-ray reflectivity has increased by about 30% as compared to its value above  $T_{mono}$  - as one would expect from Fig. 2a for the change from regime I to regime II at that  $q_z$ -position. While heating, we observed the inverse behavior, the intensity decreases until it reaches its lowest value at  $T_{mono}$ . No hysteresis was observed between cooling and heating for cooling (heating) rates smaller than  $2^\circ\text{C}$  per hour. We also carried out one temperature

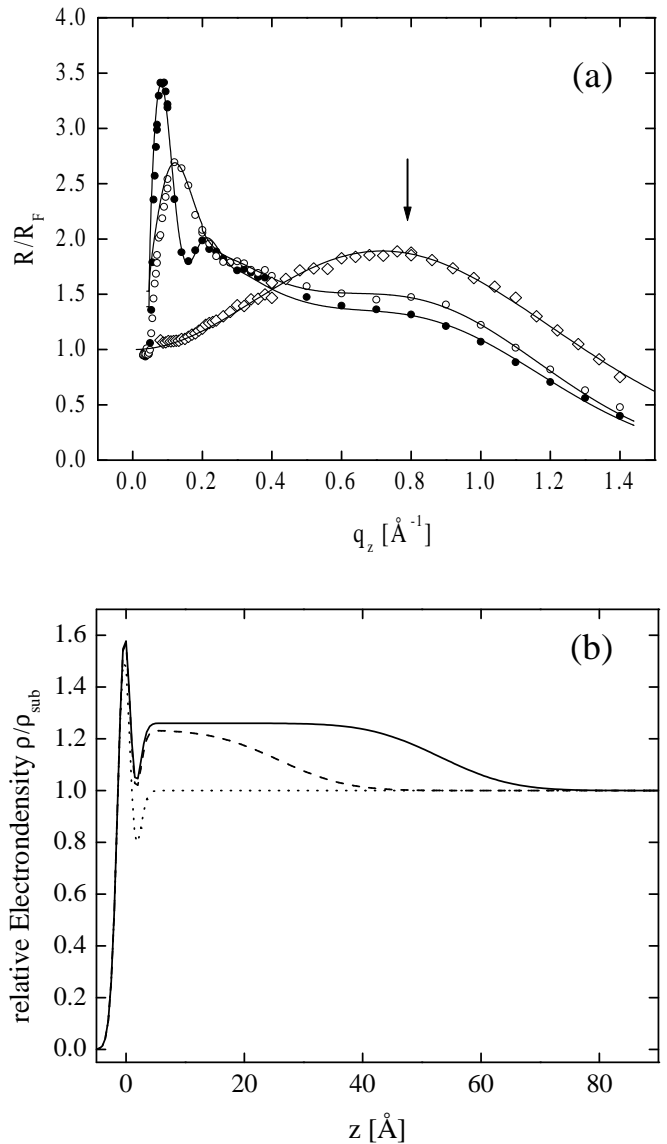


FIG. 2: (a) Fresnel normalized x-ray reflectivity  $R/R_F$  from the surface of Ga-Bi: (diamonds)  $T = 205^\circ\text{C}$ , (open circles)  $T = 220^\circ\text{C}$ , (solid circles)  $T = 222.5^\circ\text{C}$ . solid lines: fit to  $R/R_F$  with density profiles depicted in Fig. 2b. The arrow indicates the  $q_z$ -position for the temperature-dependent reflectivity measurements at fixed  $q_z = 0.8\text{\AA}^{-1}$  (T-scan) shown in Fig. 3.

(b): Electron density profiles for  $T = 205^\circ\text{C}$  (dotted line),  $T = 220^\circ\text{C}$  (dashed line) and  $T = 222.5^\circ\text{C}$  (solid line), normalized to the bulk electron density of the Ga-rich subphase.

scan with a cooling rate of  $10^\circ\text{C}$  per hour. This showed a hysteresis of  $4^\circ\text{C}$  and also the formation of a solid film at the surface. We attribute this to the expected diffusion-limited growth and the corresponding long equilibration times in such wetting geometries<sup>15</sup> and to a temperature gradient between bulk and surface rather than to an intrinsic feature of the transition.

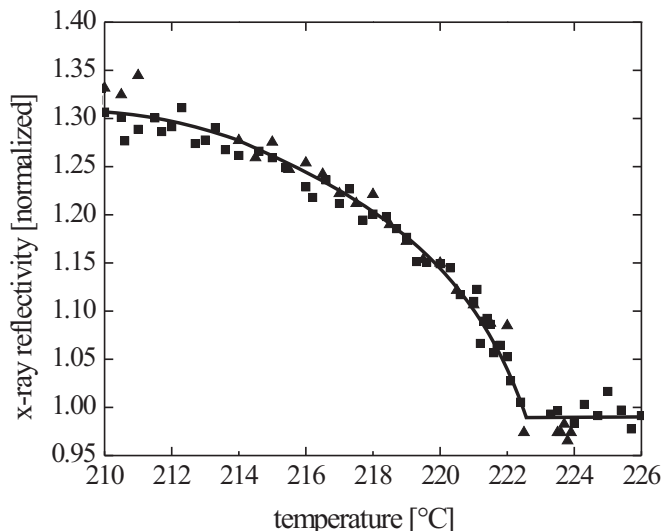


FIG. 3: temperature-dependent x-ray reflectivity at  $q_z = 0.8\text{\AA}^{-1}$  normalized to  $R/R_F$  at  $T = 222.5^\circ\text{C}$ . (squares) decreasing temperature, (triangles) increasing temperature. line: guide for the eye.

## V. CONCLUSIONS

The behavior of the reflectivity in the T-scan shows that the Bi-rich wetting film forms while approaching  $T_{mono}$  from below and vanishes in the same way on cooling, i.e. without hysteresis. Hence, the surface sensitive x-ray reflectivity measurements suggest that the first order bulk transition at the monotectic point drives a continuous structural transition at the surface. A similar behavior has been reported for Ga-Pb, a system with an analogous phase diagram (monotectic point + consolute point), by Wynblatt and Chatain<sup>4</sup>. The topology of the phase diagram of Ga-Bi forces the approach of the liquid-liquid coexistence line at  $T_{mono}$  from off coexistence while heating. Conversely, it enforces a path leading off coexistence while cooling below  $T_{mono}$  - see arrows in Fig. 1. Therefore, as Dietrich and Schick<sup>18</sup> have pointed out, one measures along a path that probes a complete wetting scenario (according to the wetting nomenclature). Since the path ends in the monotectic point with its four phase coexistence, the phenomenon is readily described as a complete wetting at a tetra point of four-phase coexistence. It should, however, be noted that  $T_{mono}$  is not the wetting temperature,  $T_w$  of the liquid-liquid system.  $T_w$  is defined as the temperature where the formation of the wetting film can be observed on coexistence between the two liquids. This temperature has to be below  $T_{mono}$ , but it

would be experimentally accessible only if the pure Bi can be supercooled sufficiently to reach the liquid-liquid coexistence, albeit in a metastable condition.

The observed transition at the surface is closely related to triple point wetting phenomena<sup>16</sup> which have been extensively studied for one component systems like Krypton on graphite<sup>17</sup>. There, one observes that the liquid wets the interface between substrate and vapor, while the solid does not. Hence, there is a wetting transition pinned at the bulk triple point  $T_3$ . In the triple point wetting scenario one walks off the liquid-vapor coexistence line following the solid-vapor sublimation line.

Another aspect of the wetting behavior close to the monotectic point is the possible nucleation of solid Bi at the surface while cooling below  $T_{mono}$ . Systematic studies on that aspect were reported only recently for different Ga-Bi alloys, concluding that Ga-Bi shows a phenomenon that can be described as surface freezing. The free surface acts as substrate for wetting of the liquid by the forming solid Bi<sup>19,20</sup>. We did also observe the formation of solid Bi at the surface while cooling below  $200^\circ\text{C}$ , but we could not study this effect in detail, since the forming solid film destroyed the flat surface of the liquid sample hampering further reflectivity measurements.

A more detailed experimental study of the wetting transition at  $T_{mono}$  has already been performed<sup>14</sup>. It has revealed the evolution of the thick film via intermediate film structures dominated by strong concentration gradients - as reported here for  $T = 220^\circ\text{C}$ . This behavior is in agreement with density functional calculations for wetting transitions of binary systems at hard walls<sup>21</sup>, which also reveal concentration gradients. Conversely, the study shows that the liquid vapor interface of a metal system acts not only as a hard wall for one component systems<sup>22</sup> forcing the ions into ordered layers parallel to that surface<sup>23,24</sup>, but also affects other structure and thermodynamic phenomena at the surface, e.g. the wetting behavior in a binary liquid metal system discussed here.

## VI. ACKNOWLEDGMENTS

This work was supported by the U.S. DOE Grant No. DE-FG02-88-ER45379, National Science Foundation Grant NSF-DMR-98-72817, and the U.S.-Israel Binational Science Foundation, Jerusalem. Brookhaven National Laboratory is supported by U.S. DOE Contract No. DE-AC02-98CH10886. P. Huber acknowledges support from the Deutsche Forschungsgemeinschaft.

<sup>1</sup> J.W. Cahn, J. Chem. Phys. 66 (1977) 3667

<sup>2</sup> S. Dietrich, in C. Domb and J.L. Lebowitz (Eds.), Phase

Transitions and Critical Phenomena, Vol. 12, Academic Press, NY, 1988

- <sup>3</sup> B.M. Law, Progress in Surface Science 66 (2001) 159
- <sup>4</sup> D. Chatain, P. Wynblatt, Surface Science 345 (1996) 85
- <sup>5</sup> H. Shim, P. Wynblatt, D. Chatain, Surface Science 476 (2001) L273
- <sup>6</sup> D. Nattland, S.C. Müller, P.D. Poh, W. Freyland, J. Non-Crystalline Solids 207 (1996) 772
- <sup>7</sup> N. Lei, Z.Q. Huang, S.A. Rice, J. Chem. Phys. 104 (1996) 4802
- <sup>8</sup> H. Tostmann, E. DiMasi, O.G. Shpyrko, P.S. Pershan, B.M. Ocko, M. Deutsch, Phys. Rev. Lett. 84 (2000) 4385
- <sup>9</sup> P. Predel, Z. f. Phys. Chem. Neue Folge 24 (1960) 206
- <sup>10</sup> P.G. De Gennes, Rev. Mod. Phys. 57 (1985) 827
- <sup>11</sup> P. S. Pershan and J. Als-Nielsen, Phys. Rev. Lett. 52 (1984) 759
- <sup>12</sup> L. G. Parratt, Physical Review 95 (1954) 359
- <sup>13</sup> B.M. Ocko, X.Z. Wu, E.B. Sirota, S.K. Sinha, M. Deutsch, Phys. Rev. Lett. 72 (1994) 242
- <sup>14</sup> P. Huber, O.G. Shpyrko, P.S. Pershan, H. Tostmann, E. DiMasi, B.M. Ocko, M. Deutsch, in preparation
- <sup>15</sup> R. Lipowsky and D. A. Huse, Phys. Rev. Lett. 57 (1986) 353
- <sup>16</sup> R. Pandit and M. E. Fisher, Phys. Rev. Lett. 51 (1983) 1772
- <sup>17</sup> G. Zimmerli, M.H.W. Chan, Phys. Rev. Lett. 45 (1992) 9347
- <sup>18</sup> S. Dietrich and M. Schick, Surface Science 382 (1997) 178
- <sup>19</sup> C. Wang, D. Nattland, W. Freyland, J. Phys.-Condensed Matter 12 (2000) 6121
- <sup>20</sup> A. Turchanin, D. Nattland, W. Freyland, Chem. Phys. Lett. 337 (2001) 5
- <sup>21</sup> H.T. Davis, Statistical Mechanics of Phases, Interfaces and Thin Films, Wiley-VCH, NY (1996)
- <sup>22</sup> J. G. Harris, J. Gryko, and S. A. Rice, Journal of Chemical Physics 87 (1987) 3069
- <sup>23</sup> O. M. Magnussen, B. M. Ocko, M. J. Regan, K. Penanen, P.S. Pershan, M. Deutsch, Phys. Rev. Lett. 74 (1995) 4444
- <sup>24</sup> M. J. Regan, E. H. Kawamoto, S. Lee, P.S. Pershan, N. Maskil, M. Deutsch, O.M. Magnussen, B. M. Ocko, L.E. Berman, Phys. Rev. Lett. 75 (1995) 2498